Ground state of the two-dimensional attractive Fermi gas:
Essential properties from few to many body

Lukas Rammelmüller,[1,2,*] William J. Porter,[2,†] and Joaquín E. Drut[2,‡]

[1]*Institute of Solid State Physics, Vienna University of Technology, A-1040 Vienna, Austria*
[2]*Department of Physics and Astronomy, University of North Carolina, Chapel Hill, North Carolina 27599, USA*
(Received 9 December 2015; published 21 March 2016)

We calculate the ground-state properties of unpolarized two-dimensional attractive fermions in the range from few to many particles. Using first-principles lattice Monte Carlo methods, we determine the ground-state energy, Tan's contact, momentum distribution, and single-particle correlation function. We investigate those properties for systems of $N = 4, 8, \ldots, 40$ particles and for a wide range of attractive couplings. As the attractive coupling is increased, the thermodynamic limit is reached at progressively lower N due to the dominance of the two-body sector. At large momenta k, the momentum distribution displays the expected k^{-4} behavior, but its onset shifts from $k \simeq 1.8 k_F$ at weak coupling towards higher k at strong coupling.

I. INTRODUCTION

Precise experiments with ultracold atomic fermion clouds are currently being carried out by several groups around the world. Among the systems in the ever-expanding set that such experiments can study, it is now possible to probe two-dimensional (2D) physics in a clean and controllable way [1–3]. This is an exciting opportunity to understand key aspects of few- and many-body quantum physics that are not specific to atoms but which are generic to 2D quantum mechanics.

Such phenomena include the classical scale invariance displayed by nonrelativistic fermions in 2D, which is broken by quantum fluctuations (i.e., the symmetry is anomalous; see Ref. [4]), a property shared with four-dimensional gauge theories like quantum chromodynamics [5]. Although finite-temperature symmetry-breaking transitions are not possible for continuous symmetries in 2D (as explained by the Mermin-Wagner theorem [6]), attractive interactions do result in a Berezinskii-Kosterlitz-Thouless (BKT) transition into a low-temperature superfluid phase [7], which is another feature generic to 2D systems. High-temperature superconductivity is also understood to be essentially a 2D phenomenon [8], and it shares with ultracold atoms the so-called pseudogap regime [9]. Last, but not least, the recent excitement about the physics of graphene is also associated with scale-invariant 2D systems and its affinity with relativistic strongly coupled matter [10].

Thus, the realization and exploration of flat ultracold atomic clouds impacts a wide range of areas in physics, and in the past few years this research has been pursued vigorously (see Refs. [11,12] for recent wide-audience reports). On the experimental side, two-dimensional fermionic clouds were first achieved just a few years ago in Refs. [13,14], and many properties, ranging from spectroscopy to thermodynamics and hydrodynamic response, have been studied since [15–28].

On the theory side, early work in 2D used mean-field approaches to study the crossover between Bose-Einstein condensation (BEC) and Bardeen-Cooper-Schrieffer (BCS)

pairing [29–31]. The ground-state energy and contact were computed in the thermodynamic limit in Ref. [32] using the diffusion Monte Carlo method, which was updated and expanded by Refs. [33,34] with a precise ab initio study of multiple ground-state properties. Studies at finite temperature have also appeared (see, e.g., Refs. [35–44]).

Thus, a fair amount is known about the many-body physics of these systems; however, much less is known about their few-body properties and how they approach the thermodynamic regime. In this work, we calculate from first principles some of the most important ground-state properties characterizing this few-to-many crossover: the energy, Tan's contact, the momentum distribution, and the single-particle propagator.

II. HAMILTONIAN AND COMPUTATIONAL APPROACH

Since our intent is to focus on nonrelativistic Fermi systems with short-range interactions, our Hamiltonian is given by

$$\hat{H} = \hat{T} + g \hat{V}, \tag{1}$$

where the kinetic and potential terms $\hat{T}$ and $\hat{V}$ are given by

$$\hat{T} = \sum_{s=\uparrow,\downarrow} \int d^2x \, \hat{\psi}_s^\dagger(\boldsymbol{x}) \left(-\frac{\hbar^2 \nabla^2}{2m} \right) \hat{\psi}_s(\boldsymbol{x}) \tag{2}$$

and

$$\hat{V} = -\int d^2x \, \hat{n}_\uparrow(\boldsymbol{x}) \hat{n}_\downarrow(\boldsymbol{x}), \tag{3}$$

respectively, and where the spin-s fermionic field operators are denoted with $\hat{\psi}_s$ and $\hat{\psi}_s^\dagger$, with associated densities $\hat{n}_s$. From this point on, we use units such that $\hbar = m = k_B = 1$, such that g is dimensionless and $\hat{V}$ has dimensions of energy as written. Although no new dimensionful parameters enter the dynamics of the system when the interaction is turned on, the classical scale invariance is broken by quantum fluctuations, which result in a nonzero pair binding energy.

Given a stable many-body system, ground-state expectation values may be obtained from the large-imaginary-time properties of an arbitrary trial state $|\phi_0\rangle$, so long as the latter is not orthogonal to the system's true ground state. In this work, we take $|\phi_0\rangle$ to be a single Slater determinant made out

---
*lukas.rammelmueller@tuwien.ac.at
†wjporter@live.unc.edu
‡drut@email.unc.edu

of the lowest-energy plane-wave orbitals. While this choice can certainly be optimized, we find it to be sufficient for our purposes.

For an operator $\hat{O}$, we define

$$O_\beta \equiv \frac{\langle \phi_0 | \, \hat{U}(\beta, \beta/2) \, \hat{O} \, \hat{U}(\beta/2, 0) \, | \phi_0 \rangle}{\langle \phi_0 | \, \hat{U}(\beta, 0) \, | \phi_0 \rangle}, \qquad (4)$$

where

$$\hat{U}(\tau_b, \tau_a) \equiv \exp[-(\tau_b - \tau_a)\hat{H}] \qquad (5)$$

is the imaginary-time evolution operator. It follows immediately that $O_\beta \xrightarrow{\beta \to \infty} \langle \hat{O} \rangle$, where the expectation value on the right is in the true ground state of the system. For some observables, in particular the Hamiltonian itself, this convergence can be easily shown to be monotonic in β (in fact, exponential), which makes their acquisition to some extent straightforward.

To address the interaction, we approximate the imaginary-time evolution operators $\hat{U}$ via a symmetric Suzuki-Trotter decomposition as

$$\hat{U}(\tau_a + \tau, \tau_a) = e^{-\tau \hat{T}/2} \, e^{-\tau g \hat{V}} \, e^{-\tau \hat{T}/2} + O(\tau^3), \qquad (6)$$

again splitting the Hamiltonian into its relatively simple one-body kinetic term and comparatively complicated two-body, zero-range potential term. While continuous-time approaches have been known for a long time [45], they have not yet been adapted to the hybrid Monte Carlo technique, which we prefer in order to make contact with lattice-QCD methods [46]. At each time step, we decompose the central (potential energy, two-body) operator via a Hubbard-Stratonovich transformation [47] into a linear combination of products of one-body operators, writing (generically)

$$e^{-\tau g \hat{V}} = \int \mathcal{D}\sigma \, e^{-\tau \hat{V}_{\uparrow,\sigma}} e^{-\tau \hat{V}_{\downarrow,\sigma}}, \qquad (7)$$

for an auxiliary field $\sigma(\boldsymbol{x})$ summed over all possible configurations at each imaginary-time slice. The specific form of the operators $e^{-\tau \hat{V}_{s,\sigma}}$, for $s = \uparrow, \downarrow$, depends on the choice of Hubbard-Stratonovich transformation. In our case, we have decoupled the interaction in the density-density channel using a continuous and compact auxiliary field (see, e.g., Ref. [48] for further details).

In the above, we have implicitly assumed that the number of spatial degrees of freedom at each time step is finite. We accomplish this by taking space to be a square lattice, which results in a lattice field theory approach in the same usual fashion as in lattice-QCD and Hubbard-model Monte Carlo calculations. The field integral of Eq. (7) is estimated in practice using Metropolis-algorithm-based Monte Carlo methods, which is possible as for unpolarized systems there is no sign problem. Further details can be found in Ref. [48]; closely related methods were used to examine systems in one dimension (1D) in Ref. [49] and in three dimensions (3D) in Ref. [50].

In this work, we have used spatial lattice sizes of side $N_x = 24, 28, 32, 36, 40$ points, and taken the spatial lattice spacing to be $\ell = 1$ and the temporal lattice spacing τ such that $\tau/\ell^2 = 0.01$–0.05. While the method is not limited by these parameters, we found them sufficient to achieve the continuum

limit and to characterize the crossover from few- to many-body physics. On the other hand, the Monte Carlo estimation of the field integrals carries a statistical uncertainty. To reduce the latter, we took at least 500 decorrelated samples of the auxiliary field, such that the uncertainty can be expected to be of order 5% or less.

III. RESULTS AND DISCUSSION

To calibrate our lattice field theory, we solved the two-body problem for all values of N_x mentioned above and determined the lattice binding energy ε_B as a function of the dimensionless coupling g and the lattice size N_x. Using those results, we performed calculations for higher particle numbers $N = 4, 8, 12, \ldots, 40$ at fixed physics as set by the renormalized coupling $\eta = 1/2 \ln(2\varepsilon_F/\varepsilon_B)$, where $\varepsilon_F = k_F^2/2$ is the Fermi energy, $k_F = \sqrt{2\pi n}$ is the Fermi momentum, and $n = N/L^2$ is the total density. To ensure that our results are converged to the ground state, we followed the procedure outlined above of calculating at finite β and extrapolating to $\beta \to \infty$.

In Fig. 1, we show our results for the energy (extrapolated to infinite volume), in units of the energy of the noninteracting case $E_{FG} = \frac{1}{2}N\varepsilon_F$, as a function of particle number and coupling. For display purposes, we have separated weak
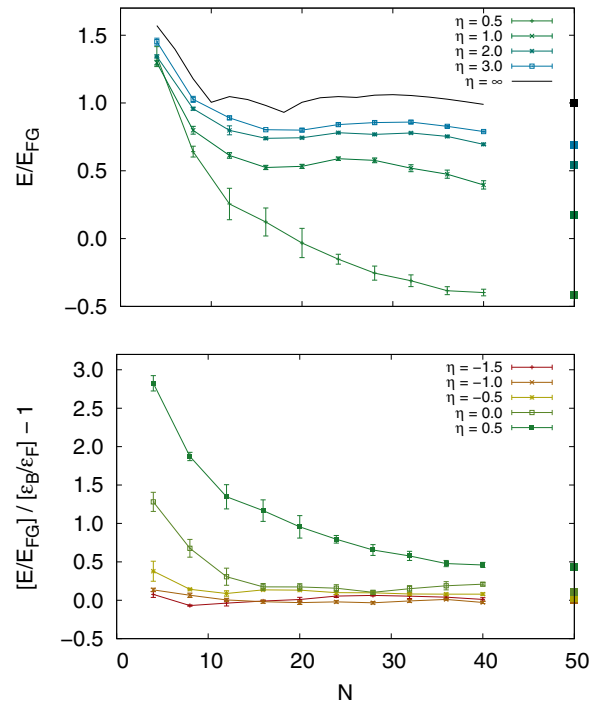

FIG. 1. Ground-state energy E of $N = 4, 8, 12, \ldots, 40$ unpolarized fermions, for several values of the dimensionless coupling $\eta = -1.5, -1.0, \ldots, 3.0, \infty$, the final corresponding to a free system. Top panel shows E for the four weakest couplings we calculated, in units of the energy of the noninteracting system $E_{FG} = \frac{1}{2}N\varepsilon_F$. Bottom panel displays E for the strongest couplings we considered, using the binding energy per particle $\varepsilon_B/2$ as a scale. Clearly, for $\eta < 0$ the energy per particle is dominated by the pair binding energy across all particle numbers. In both plots, the ground-state energy results of Ref. [33] in the thermodynamic limit are shown with solid squares at $N = 50$.
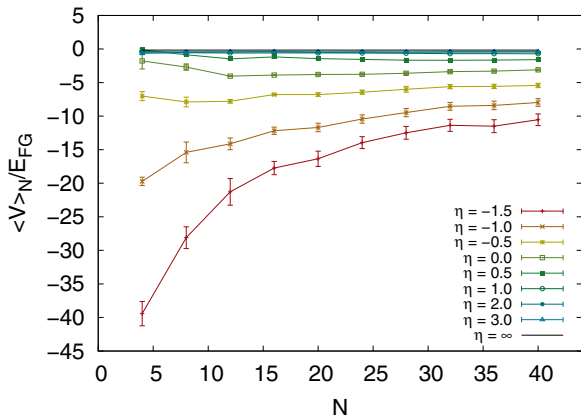
FIG. 2. Expectation value of the interaction operator $\hat{V}$ for $N = 4, 8, 12, \ldots, 40$ fermions, in units of the ground-state energy of the noninteracting gas, for several values of the dimensionless coupling $\eta = -1.5, -1.0, \ldots, 3.0$, along with the noninteracting case $\eta \to \infty$. The solid line shows $-1/(2\pi)$, which is the result in the noninteracting limit.

couplings (i.e., BCS side, shown in the top panel) from strong couplings (mostly BEC side, shown in the bottom panel). As evident from the top panel, at weak couplings there is a structure of oscillations before the few-body problems heal to the thermodynamic limit result (shown on the right side of the figure with squares, using the data of Ref. [33] and interpolations thereof where needed). Such oscillations are typically associated with so-called shell effects and have been seen in 1D and 3D analogues of this system (see, e.g., Refs. [51] and [52]). In order to better understand the strong coupling regime, we subtracted the binding energy per particle $\varepsilon_B/2$ from the total energy per particle in the bottom panel. Indeed, for $\eta \leqslant 1.0$, the onset of the BEC regime implies that the energy is expected to be dominated by the binding energy of the pairs, which form immediately upon turning on the interaction. The numerical results plotted in Fig. 1 are given in Appendix B, Table II.
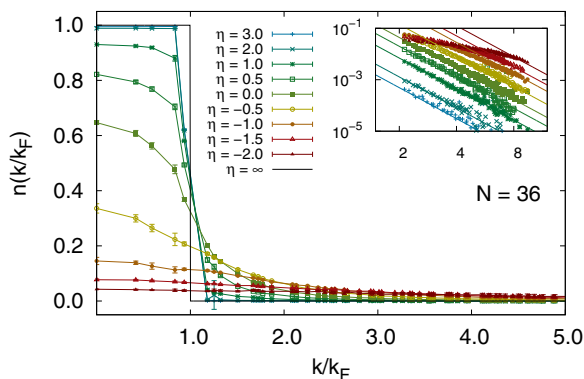
While the ground-state energy is an essential quantity in any few- and many-body problem, more detailed information about the short-distance behavior of the system can be obtained from Tan's contact C [53]. Indeed, it has been shown that C controls the high-momentum tail of the momentum distribution (see below) [54], as well as multiple sum rules of real-time response functions [55]. The calculation of C itself, however, involves a many-body problem that requires computational approaches [51,56]. The contact obeys an adiabatic theorem (see Refs. [57,58]), which indicates that C is proportional to the change in the ground-state energy E with the s-wave scattering length a_0. In our Hamiltonian Eq. (1), the scattering length enters fully through the bare coupling g (and, of course, the UV lattice cutoff, which we hold constant). Therefore,

$$C \propto \frac{\partial E}{\partial \ln(k_F a_0)} = \frac{\partial E}{\partial g} \frac{\partial g}{\partial \ln(k_F a_0)}. \tag{8}$$

The factor $\partial g/\partial \ln(k_F a_0)$ is a derivative at constant N that depends only on two-body physics, as the bare coupling g is determined by tuning to the desired a_0 by solving the two-body problem. The $\partial E/\partial g$ factor, on the other hand, encodes many-body correlations and depends on the particle content N. Because we have used a contact interaction [see Eq. (1)], the expectation value of the potential energy gives us access to $\partial E/\partial g$ through the Hellmann-Feynman relation for the N-body problem:

$$\langle \hat{V} \rangle_N = \frac{\partial E}{\partial g}. \tag{9}$$

In Fig. 2, we show $\langle \hat{V} \rangle_N$ in units of the ground-state energy of the noninteracting gas E_{FG} and as a function of both particle number and coupling. The numerical results plotted here are given in Appendix B, Table III.

In Fig. 3, we show our results for the momentum distribution as a function of k/k_F for $N = 36$ particles and for several values of the dimensionless coupling η, extrapolated to $\beta \to \infty$ (i.e., the ground state). Data at finite β are shown in Appendix A. The inset shows the same data in log-log form along with fits of the expected power law k^{-4} (see, e.g., Ref. [59]), which yield the contact at $k \gg k_F$. The expected
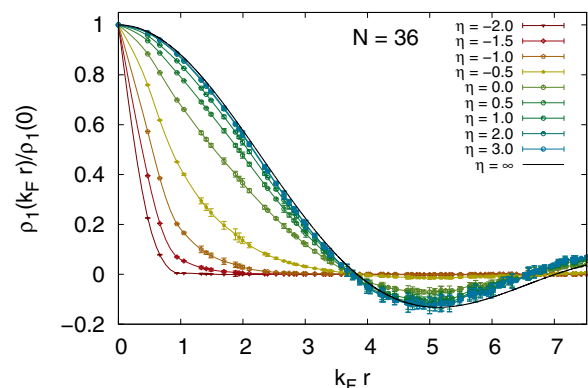

FIG. 3. Momentum distribution of $N = 36$ unpolarized fermions, as a function of k/k_F, for several values of the dimensionless coupling $\eta = -2.0, -1.5, \ldots, 3.0$, as well as the noninteracting case. Inset: Momentum distribution in log-log scale, showing the power-law decay that heals to a $\sim (k/k_F)^{-4}$ decrease at large k.

FIG. 4. One-body density matrix ρ_1 for $N = 36$ unpolarized fermions, as a function of $k_F r$, for several values of the dimensionless coupling $\eta = -2.0, \ldots, 3.0$, along with the $\eta \to \infty$ (i.e., noninteracting) case.

TABLE I. Fit parameter a obtained by fitting Eq. (11) to the data of Fig. 4, as a function of the dimensionless coupling η. The rightmost column shows the sum of the absolute value of the residuals per degree of freedom. These values of a exemplify the typical numbers obtained across all particle numbers, i.e., beyond the data of Fig. 4.

η	a	Mean residual
−2.0	0.45(3)	0.001
−1.5	0.44(3)	0.002
−1.0	0.42(3)	0.004
−0.5	0.27(6)	0.03
0.0	0.11(4)	0.02
0.5	0.06(4)	0.02
1.0	0.05(7)	0.02
2.0	0.0(1)	0.02
3.0	0.0(1)	0.02

behavior is obtained at weak coupling, but the region where it is valid becomes increasingly limited (i.e., it moves toward high k/k_F at strong coupling. Thus, in order to see the expected momentum tail at strong coupling, calculations at larger volumes (lower k_F) are needed. For most of the couplings we studied, however, it appears that the k^{-4} decay is reached around $k/k_F \simeq 1.8 - 2.0$, which is remarkably close to its 3D counterpart [56].

In Fig. 4, we show our results for the one-body density matrix ρ_1 defined in our unpolarized system as

$$\rho_1(\boldsymbol{x},\boldsymbol{x}') = \langle \hat{\psi}_\uparrow^\dagger(\boldsymbol{x})\hat{\psi}_\uparrow(\boldsymbol{x}')\rangle = \langle \hat{\psi}_\downarrow^\dagger(\boldsymbol{x})\hat{\psi}_\downarrow(\boldsymbol{x}')\rangle, \quad (10)$$

given the figure as a function of the dimensionless distance $k_F r$, where $r = |\boldsymbol{x} - \boldsymbol{x}'|$, as we take into account translation and rotation invariance. The results shown are for $N = 36$ particles and cover several values of the coupling η. The localized shape of ρ_1 around $x = 0$ at strong couplings is a direct manifestation of the formation of bound pairs, which in turn makes lattice approaches to the problem more challenging: The presence of the lattice-spacing scale competes with the pair size, which must be properly resolved in order to obtain accurate results.

To encode the intermediate and short-distance ($k_F r < 3.0$) shape of our numerical results for ρ_1, we fit the following

FIG. 6. Extrapolation to the infinite volume limit for $N = 16,32$ unpolarized fermions at fixed dimensionless coupling $\eta = 1.0$, as a function of N_x^{-2}.

dimensionless form to the data of Fig. 4:

$$f(k_F r,\eta) = 2\,e^{-a\,p_B r}\,\frac{J_1(k_F r)}{k_F r}, \quad (11)$$

where a is a fit parameter used to interpolate across couplings, and $p_B = \sqrt{2}k_F e^{-\eta}$ is the binding momentum of the two-body system (see Table I for fit results). The exponential factor in Eq. (11) is motivated by the deep bound state in the BEC regime, where single-particle correlation lengths are expected to be governed by the inverse binding momentum. The Bessel function factor, along with the denominator, corresponds to the noninteracting case in the continuum limit.

IV. SUMMARY AND CONCLUSIONS

In this work, we set out to examine, in a fully nonperturbative fashion, the progression from few- to many-body fermions in 2D, with attractive short-range interactions across a wide range of coupling strengths in the BEC-BCS crossover. Using lattice Monte Carlo methods akin to those of lattice QCD, we calculated the universal behavior of systems of $N = 4,8,\ldots,40$ particles in the ground state. We focused, in particular, on the energy per particle, Tan's contact, the momentum distribution, and the single-particle correlator. The
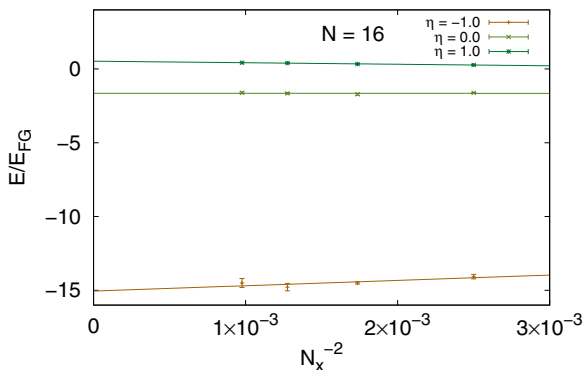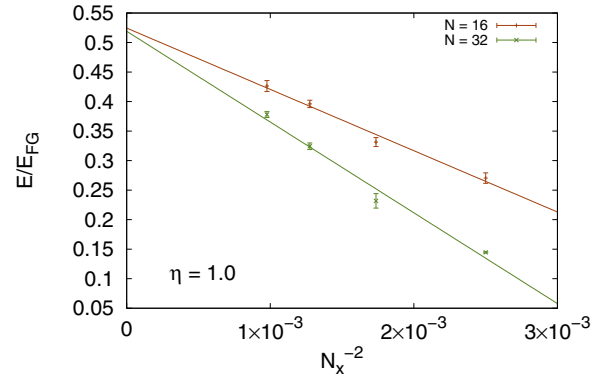

FIG. 5. Extrapolation to the infinite volume limit for $N = 16$ unpolarized fermions, as a function of N_x^{-2}, for several values of the dimensionless coupling $\eta = -1.0, 0.0, 1.0$.
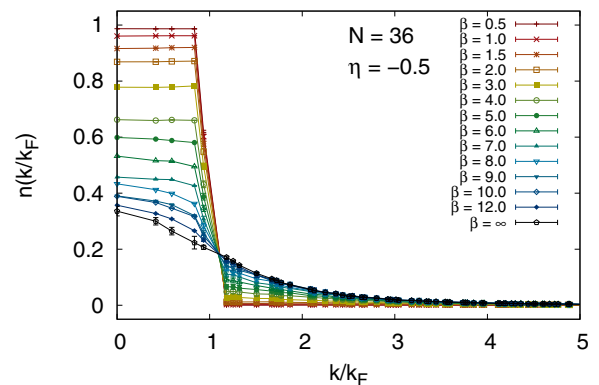

FIG. 7. Momentum distribution extrapolated to infinite imaginary time β for $N = 36$ unpolarized fermions on a 32×32 lattice and at fixed dimensionless coupling $\eta = -0.5$.

TABLE II. Ground-state energy E on the lattice, in units of the continuum noninteracting energy $E_{\text{FG}} = N\varepsilon_F/2$ of the N-particle system, as a function of N and the dimensionless coupling η.

	η								
N	-1.5	-1.0	-0.5	0.0	0.5	1.0	2.0	3.0	∞
4	$-37(2)$	$-12.8(3)$	$-3.4(7)$	$0.6(2)$	$1.34(7)$	$1.30(2)$	$1.34(1)$	$1.45(3)$	$\pi/2$
8	$-43.0(3)$	$-13.8(4)$	$-4.66(5)$	$-0.6(2)$	$0.64(4)$	$0.80(3)$	$0.96(1)$	$1.03(2)$	$3\pi/8$
12	$-41(2)$	$-14.7(3)$	$-5.0(2)$	$-1.4(2)$	$0.3(1)$	$0.61(2)$	$0.80(3)$	$0.89(1)$	$4\pi/12$
16	$-40.6(2)$	$-15.0(3)$	$-4.70(4)$	$-1.65(9)$	$0.1(1)$	$0.52(2)$	$0.74(1)$	$0.80(0)$	$5\pi/16$
20	$-39(1)$	$-15.2(4)$	$-4.72(6)$	$-1.65(9)$	$-0.0(1)$	$0.53(2)$	$0.74(1)$	$0.80(1)$	$8\pi/25$
24	$-38.0(8)$	$-15.1(2)$	$-4.9(1)$	$-1.69(9)$	$-0.15(4)$	$0.59(1)$	$0.78(0)$	$0.84(1)$	$4\pi/12$
28	$-37.6(3)$	$-15.3(2)$	$-4.91(8)$	$-1.79(4)$	$-0.25(5)$	$0.58(2)$	$0.77(1)$	$0.86(1)$	$33\pi/98$
32	$-38(1)$	$-14.9(3)$	$-4.99(1)$	$-1.70(8)$	$-0.31(4)$	$0.52(3)$	$0.78(1)$	$0.86(1)$	$43\pi/128$
36	$-38.5(6)$	$-14.6(1)$	$-5.01(7)$	$-1.6(1)$	$-0.38(3)$	$0.48(3)$	$0.75(1)$	$0.82(0)$	$53\pi/162$
40	$-39.8(9)$	$-15.2(2)$	$-5.00(9)$	$-1.58(4)$	$-0.40(2)$	$0.40(3)$	$0.70(0)$	$0.80(1)$	$63\pi/200$

ground-state energy for each coupling strength forms a smooth curve with mild oscillations toward the thermodynamic limit. For $\eta \leqslant 0$, particularly for $N > 16$, the ground-state energy is completely dominated by the binding energy of the pairs. Thus, the thermodynamic limit is reached much faster on the BEC side than on the BCS side. The momentum distribution approaches a $(k/k_F)^{-4}$ decay at large k, as expected, but the onset of that behavior shifts noticeably towards large k as the coupling is increased. Finally, our fits to the single-particle correlation function ρ_1 indicate a shift from a k_F-dominated region at weak coupling to a p_B-dominated region at strong coupling.

APPENDIX A: FINITE-VOLUME EFFECTS AND EXTRAPOLATIONS

In this appendix we elaborate on the procedure we employed to carry out extrapolations to the infinite volume

limit, and present specific examples. In Fig. 5 we show the extrapolation for $N = 16$ particles for three different values of the dimensionless coupling η. To complement that example, we show in Fig. 6 the infinite-volume extrapolation for two different particle numbers at a fixed coupling.

In Fig. 7 we show, for a specific coupling $\eta = -0.5$, the results of extrapolating our data for the momentum distribution $n(k)$ to the ground state, which we accomplish by increasing the length β of the imaginary time direction (i.e., the projection time). Clearly, such a coupling, though intermediate in strength, requires $\beta \simeq 8.0$ to start converging to the large β limit, in particular for the region $k < k_F$. One way to overcome such large projection times is to use a different guess for the ground-state wave function, as done for instance in Refs. [33,34].

APPENDIX B: GROUND-STATE DATA TABLES

In this appendix we present tables showing our estimates for the ground-state energy and Tan's contact as a function of the coupling $\eta = -1.5, -1.0, \ldots, 3.0$, for particle numbers $N = 4, 8, 12, \ldots, 40$, extrapolated to the infinite-volume limit.

TABLE III. Ground-state interaction $\langle \hat{V} \rangle_N$, in units of the energy of the noninteracting gas E_{FG}, as a function of N and the dimensionless coupling η.

	η								
N	-1.5	-1.0	-0.5	0.0	0.5	1.0	2.0	3.0	∞
4	$-39(2)$	$-19.7(6)$	$-7.0(7)$	$-1(1)$	$-0.1(2)$	$-0.34(5)$	$-0.50(1)$	$-0.6(2)$	$-1/(2\pi)$
8	$-28(2)$	$-15(1.5)$	$-7.9(7)$	$-2.7(5)$	$-0.86(9)$	$-0.55(9)$	$-0.41(1)$	$-0.5(1)$	$-1/(2\pi)$
12	$-21(2)$	$-14.1(9)$	$-7.8(3)$	$-4.0(1)$	$-1.47(4)$	$-0.59(1)$	$-0.42(4)$	$-0.44(7)$	$-1/(2\pi)$
16	$-17.7(1)$	$-12.2(5)$	$-6.8(1)$	$-3.9(1)$	$-1.2(2)$	$-0.58(1)$	$-0.38(2)$	$-0.43(2)$	$-1/(2\pi)$
20	$-16(1)$	$-11.7(6)$	$-6.8(3)$	$-3.8(1)$	$-1.44(8)$	$-0.59(4)$	$-0.41(2)$	$-0.52(6)$	$-1/(2\pi)$
24	$-14.0(9)$	$-10.4(6)$	$-6.4(3)$	$-3.8(1)$	$-1.55(1)$	$-0.60(1)$	$-0.41(1)$	$-0.50(5)$	$-1/(2\pi)$
28	$-12.5(9)$	$-9.5(6)$	$-6.0(4)$	$-3.6(2)$	$-1.67(3)$	$-0.64(1)$	$-0.44(1)$	$-0.48(5)$	$-1/(2\pi)$
32	$-11.4(9)$	$-8.5(6)$	$-5.6(3)$	$-3.4(1)$	$-1.68(1)$	$-0.69(4)$	$-0.41(1)$	$-0.46(4)$	$-1/(2\pi)$
36	$-11.5(1)$	$-8.4(6)$	$-5.6(3)$	$-3.3(1)$	$-1.65(1)$	$-0.68(3)$	$-0.40(2)$	$-0.45(4)$	$-1/(2\pi)$
40	$-10.5(9)$	$-8.0(6)$	$-5.4(3)$	$-3.1(1)$	$-1.59(2)$	$-0.71(3)$	$-0.41(2)$	$-0.43(3)$	$-1/(2\pi)$

[1] Ultracold Fermi Gases, Proceedings of the International School of Physics "Enrico Fermi", Course CLXIV, Varenna, June 20–30, 2006, edited by M. Inguscio, W. Ketterle, C. Salomon (IOS Press, Amsterdam, 2008).

[2] I. Bloch, J. Dalibard, and W. Zwerger, Rev. Mod. Phys. **80**, 885 (2008); S. Giorgini, L. P. Pitaevskii, and S. Stringari, *ibid.* **80**, 1215 (2008).

[3] J. Levinsen and M. M. Parish, Ann. Rev. Cold Atoms Mol. **3**, 1 (2015).

[4] J. Hofmann, Phys. Rev. Lett. **108**, 185303 (2012); E. Taylor and M. Randeria, *ibid.* **109**, 135301 (2012); **110**, 089904(E) (2013).

[5] J. R. Ellis, Nucl. Phys. B **22**, 478 (1970); R. J. Crewther, Phys. Lett. B **33**, 305 (1970); M. S. Chanowitz and J. R. Ellis, *ibid.* **40**, 397 (1972); J. Schechter, Phys. Rev. D **21**, 3393 (1980); J. C. Collins, A. Duncan, and S. D. Joglekar, *ibid.* **16**, 438 (1977); N. K. Nielsen, Nucl. Phys. B **120**, 212 (1977).

[6] N. D. Mermin and H. Wagner, Phys. Rev. Lett. **17**, 1133 (1966); P. C. Hohenberg, Phys. Rev. **158**, 383 (1967); S. Coleman, Commun. Math. Phys. **31**, 259 (1973).

[7] *Forty Years of Berezinskii-Kosterlitz-Thouless Theory*, edited by J. V. Jose (World Scientific, Singapore, 2013); V. L. Berezinskii, Sov. Phys. JETP **34**, 610 (1972); J. M. Kosterlitz and D. J. Thouless, J. Phys. C **6**, 1181 (1973); J. M. Kosterlitz, *ibid.* **7**, 1046 (1974).

[8] D. N. Basov and T. Timusk, Rev. Mod. Phys. **77**, 721 (2005); S. A. Kivelson, I. P. Bindloss, E. Fradkin, V. Oganesyan, J. M. Tranquada, A. Kapitulnik, and C. Howald, *ibid.* **75**, 1201 (2003).

[9] C. A. R. Sá de Melo, M. Randeria, and J. R. Engelbrecht, Phys. Rev. Lett. **71**, 3202 (1993); J. Stajic, J. N. Milstein, Q. Chen, M. L. Chiofalo, M. J. Holland, and K. Levin, Phys. Rev. A **69**, 063610 (2004); Q. Chen *et al.*, Phys. Rep. **412**, 1 (2005); K. Levin and Q. Chen, Finite Temperature Effects in Ultracold Fermi Gases, Proceedings of the International School of Physics "Enrico Fermi", edited by M. Inguscio, W. Ketterle, C. Salomon (IOS Press, Amsterdam, 2008), Vol. 164, p. 751; Y. He, C. C. Chien, Q. Chen, and K. Levin, Phys. Rev. B **76**, 224516 (2007), and earlier references therein; A. Perali, P. Pieri, L. Pisani, and G. C. Strinati, Phys. Rev. Lett. **92**, 220404 (2004).

[10] V. N. Kotov, B. Uchoa, V. M. Pereira, F. Guinea, and A. H. Castro Neto, Rev. Mod. Phys. **84**, 1067 (2012).

[11] M. Randeria, Physics **5**, 10 (2012).

[12] P. Pieri, Physics **8**, 53 (2015).

[13] K. Martiyanov, V. Makhalov, and A. Turlapov, Phys. Rev. Lett. **105**, 030404 (2010).

[14] M. Feld, B. Fröhlich, E. Vogt, M. Koschorreck, and M. Köhl, Nature (London) **480**, 75 (2011).

[15] B. Fröhlich, M. Feld, E. Vogt, M. Koschorreck, W. Zwerger, and M. Köhl, Phys. Rev. Lett. **106**, 105301 (2011).

[16] S. K. Baur, B. Fröhlich, M. Feld, E. Vogt, D. Pertot, M. Koschorreck, and M. Köhl, Phys. Rev. A **85**, 061604 (2012).

[17] P. Dyke, E. D. Kuhnle, S. Whitlock, H. Hu, M. Mark, S. Hoinka, M. Lingham, P. Hannaford, and C. J. Vale, Phys. Rev. Lett. **106**, 105304 (2011).

[18] A. T. Sommer, L. W. Cheuk, M. J. H. Ku, W. S. Bakr, and M. W. Zwierlein, Phys. Rev. Lett. **108**, 045302 (2012).

[19] Y. Zhang, W. Ong, I. Arakelyan, and J. E. Thomas, Phys. Rev. Lett. **108**, 235302 (2012); M. Koschorreck, D. Pertot, E. Vogt, B. Fröhlich, M. Feld, and M. Köhl, Nature (London) **485**, 619 (2012).

[20] A. A. Orel, P. Dyke, M. Delehaye, C. J. Vale, and H. Hu, New J. Phys. **13**, 113032 (2011).

[21] E. Vogt, M. Feld, B. Fröhlich, D. Pertot, M. Koschorreck, and M. Köhl, Phys. Rev. Lett. **108**, 070404 (2012).

[22] B. Fröhlich, M. Feld, E. Vogt, M. Koschorreck, M. Köhl, C. Berthod, and T. Giamarchi, Phys. Rev. Lett. **109**, 130403 (2012).

[23] P. Dyke, K. Fenech, T. Peppler, M. G. Lingham, S. Hoinka, W. Zhang, S. G. Peng, B. Mulkerin, H. Hu, X. J. Liu, and C. J. Vale, Phys. Rev. A **93**, 011603 (2016).

[24] V. Makhalov, K. Martiyanov, and A. Turlapov, Phys. Rev. Lett. **112**, 045301 (2014).

[25] W. Ong, C. Cheng, I. Arakelyan, and J. E. Thomas, Phys. Rev. Lett. **114**, 110403 (2015).

[26] M. G. Ries, A. N. Wenz, G. Zürn, L. Bayha, I. Boettcher, D. Kedar, P. A. Murthy, M. Neidig, T. Lompe, and S. Jochim, Phys. Rev. Lett. **114**, 230401 (2015).

[27] P. A. Murthy, I. Boettcher, L. Bayha, M. Holzmann, D. Kedar, M. Neidig, M. G. Ries, A. N. Wenz, G. Zürn, and S. Jochim, Phys. Rev. Lett. **115**, 010401 (2015).

[28] K. Fenech, P. Dyke, T. Peppler, M. G. Lingham, S. Hoinka, H. Hu, and C. J. Vale, Phys. Rev. Lett. **116**, 045302 (2016); I. Boettcher, L. Bayha, D. Kedar, P. A. Murthy, M. Neidig, M. G. Ries, A. N. Wenz, G. Zürn, S. Jochim, and T. Enss, *ibid.* **116**, 045303 (2016).

[29] K. Miyake, Prog. Theor. Phys. **69**, 1794 (1983).

[30] M. Randeria, J.-M. Duan, and L.-Y. Shieh, Phys. Rev. Lett. **62**, 981 (1989); Phys. Rev. B **41**, 327 (1990); S. Schmitt-Rink, C. M. Varma, and A. E. Ruckenstein, Phys. Rev. Lett. **63**, 445 (1989); M. Drechsler and W. Zwerger, Ann. Phys. (Leipzig) **1**, 15 (1992).

[31] W. Zhang, G.-D. Lin, and L.-M. Duan, Phys. Rev. A **77**, 063613 (2008).

[32] G. Bertaina and S. Giorgini, Phys. Rev. Lett. **106**, 110403 (2011).

[33] H. Shi, S. Chiesa, and S. Zhang, Phys. Rev. A **92**, 033603 (2015).

[34] A. Galea, H. Dawkins, S. Gandolfi, and A. Gezerlis, Phys. Rev. A **93**, 023602 (2016).

[35] X.-J. Liu, H. Hu, and P. D. Drummond, Phys. Rev. B **82**, 054524 (2010).

[36] M. Bauer, M. M. Parish, and T. Enss, Phys. Rev. Lett. **112**, 135302 (2014).

[37] V. Ngampruetikorn, J. Levinsen, and M. M. Parish, Phys. Rev. Lett. **111**, 265301 (2013).

[38] M. Barth and J. Hofmann, Phys. Rev. A **89**, 013614 (2014).

[39] C. Chafin and T. Schäfer, Phys. Rev. A **88**, 043636 (2013).

[40] S. Chiacchiera, D. Davesne, T. Enss, and M. Urban, Phys. Rev. A **88**, 053616 (2013).

[41] S. K. Baur, E. Vogt, M. Köhl, and G. M. Bruun, Phys. Rev. A **87**, 043612 (2013).

[42] T. Enss, C. Küppersbusch, and L. Fritz, Phys. Rev. A **86**, 013617 (2012).

[43] E. R. Anderson and J. E. Drut, Phys. Rev. Lett. **115**, 115301 (2015).

[44] B. C. Mulkerin, K. Fenech, P. Dyke, C. J. Vale, X.-J. Liu, and H. Hu, Phys. Rev. A **92**, 063636 (2015).

[45] S. M. A. Rombouts, K. Heyde, and N. Jachowicz, Phys. Rev. Lett. **82**, 4155 (1999).

[46] S. Duane, A. D. Kennedy, B. J. Pendleton, and D. Roweth, Phys. Lett. B **195**, 216 (1987); S. Gottlieb, W. Liu, D. Toussaint, R. L. Renken, and R. L. Sugar, Phys. Rev. D **35**, 2531 (1987).

[47] R. L. Stratonovich, Sov. Phys. Dokl. **2**, 416 (1958); J. Hubbard, Phys. Rev. Lett. **3**, 77 (1959).

[48] D. Lee, Phys. Rev. C **78**, 024001 (2008); Prog. Part. Nucl. Phys. **63**, 117 (2009); J. E. Drut and A. N. Nicholson, J. Phys. G **40**, 043101 (2013).

[49] M. D. Hoffman, P. D. Javernick, A. C. Loheac, W. J. Porter, E. R. Anderson, and J. E. Drut, Phys. Rev. A **91**, 033618 (2015).

[50] A. Bulgac, J. E. Drut, and P. Magierski, Phys. Rev. Lett. **96**, 090404 (2006); Phys. Rev. A **78**, 023625 (2008); J. E. Drut, T. A. Lähde, G. Wlazlowski, and P. Magierski, *ibid.* **85**, 051601(R) (2012).

[51] L. Rammelmüller, W. J. Porter, A. C. Loheac, and J. E. Drut, Phys. Rev. A **92**, 013631 (2015).

[52] M. M. Forbes, S. Gandolfi, and A. Gezerlis, Phys. Rev. Lett. **106**, 235303 (2011).

[53] E. Braaten, in *The BCS-BEC Crossover and the Unitary Fermi Gas*, edited by W. Zwerger (Springer-Verlag, Heidelberg, 2012); X.-J. Liu, Phys. Rep. **524**, 37 (2013).

[54] S. Tan, Ann. Phys. **323**, 2952 (2008); **323**, 2971 (2008); **323**, 2987 (2008); S. Zhang and A. J. Leggett, Phys. Rev. A **77**, 033614 (2008); E. Braaten and L. Platter, Phys. Rev. Lett. **100**, 205301 (2008); E. Braaten, D. Kang, and L. Platter, *ibid.* **104**, 223004 (2010)

[55] D. T. Son and E. G. Thompson, Phys. Rev. A **81**, 063634 (2010); E. Taylor and M. Randeria, *ibid.* **81**, 053610 (2010).

[56] J. E. Drut, T. A. Lähde, and T. Ten, Phys. Rev. Lett. **106**, 205302 (2011); K. Van Houcke, F. Werner, E. Kozik, N. Prokof'ev, and B. Svistunov, arXiv:1303.6245 (unpublished).

[57] F. Werner, Phys. Rev. A **78**, 025601 (2008); C. Langmack, M. Barth, W. Zwerger, and E. Braaten, Phys. Rev. Lett. **108**, 060402 (2012).

[58] M. Valiente, N. T. Zinner, and K. Mølmer, Phys. Rev. A **84**, 063626 (2011); **86**, 043616 (2012).

[59] F. Werner and Y. Castin, Phys. Rev. A **86**, 013626 (2012).